TECTONICS, VOL. 7, NO. 6, PAGES 1291-1306, DECEMBER 1988

EXTENSION OF THE NAJD SHEAR SYSTEM FROM SAUDI ARABIA TO THE CENTRAL EASTERN DESERT OF EGYPT BASED ON INTEGRATED FIELD AND LANDSAT OBSERVATIONS

Mohamed Sultan, Raymond E. Arvidson, and Ian J. Duncan

Department of Earth and Planetary Sciences, McDonnell Center for the Space Sciences, Washington University, St. Louis, Missouri

Robert J. Stern

Programs in Geosciences, University of Texas at Dallas, Richardson, Texas

Baher El Kaliouby

Department of Geology, Faculty of Science, Ain Shams University, Abbassia, Cairo, Egypt

Abstract. The Najd Shear System in Saudi Arabia extends over 1200 km in a NW-SE direction and has a width of approximately 300 km. A digital color mosaic, compiled from seven Landsat thematic mapper scenes, was used to delineate characteristic structural features of the Najd System in the Midyan region of Saudi Arabia and to search for similar features in the Egyptian Eastern Desert. The digital mosaic was generated using ratios of Landsat thematic mapper bands (bands 5/4 x 3/4, 5/1, 5/7) that are sensitive to the rock content of Fe-bearing aluminosilicates, spectrally opaque phases, and hydroxyl-bearing or carbonate minerals, respectively. The mosaic covers approximately 130,000 km^2 of late Proterozoic exposures of the Arabian-Nubian Shield and has the Eastern Desert and the Midyan region placed in their approximate pre-Red Sea locations. The Ajjaj Shear Zone (AJZ) marks the termination of the Najd System against the eastern margin of the Red Sea in the Midyan region. The AJZ aligns with the central Eastern Desert, based on analysis of pre-Red Sea locations. Analyses of Landsat data and field observations show that the Ajjaj Shear Zone and the central Eastern Desert exhibit the following features in common: (1) outcrops that are generally elongate in a NW-SE direction as a result of folding, with fine-scale lithologic heterogeneity at the outcrop scale related to deformation associated with faulting; (2) NW trending left-lateral faults and ductile shear zones; (3) subhorizontal, NW trending mineral lineations, and variably dipping NW trending foliations, with local changes in attitude around large competent (e.g., granitic) bodies; and (4) lithologic contacts that are generally tectonic in nature and related to faulting. These features are less common to the north and south of both the Ajjaj Shear Zone and the central Eastern Desert. Results are consistent with the Najd Shear System extending into the Eastern Desert and dominating the structural patterns within the central part of the Eastern Desert.

Paper number 88TC03204.
0278-7407/88/88TC-03204$10.00

1. INTRODUCTION

The Arabian Shield formed by the accretion of ensimatic and ensialic island arcs between 715 and 630 Ma [Stoeser and Camp, 1985](Figure 1). The Shield formed from at least five arcs, separated by four N-S or NE-SW trending ophiolite-bearing suture zones [Stoeser and Camp, 1985]. The collision-related tectonic fabric is predominantly oriented N-S or NE-SW [Moore, 1979]. The Najd Shear System (NSS) modified the earlier structures into northwesterly fabrics at about 530-630 Ma [Stacey and Agar, 1985].

The NSS of the Arabian Shield is the largest recognized pre-Mesozoic transcurrent fault system on Earth [Stern, 1985], extending in a NW-SE direction over 1200 km in outcrop, with a width of approximately 300 km [Agar, 1987]. The NSS aligns with faults in the South Yemen coast and in the Arabian Sea bed to the SE [Brown, 1972], making a potential total length in excess of 2000 km [Moore, 1979]. The main trends of the NSS terminate at the eastern margin of the Red Sea, between latitudes 26° and 27°45'N [Brown, 1970]. Along the zone occupied by the NSS in Saudi Arabia brittle and ductile styles of deformation prevail, superimpose on, and obliterate earlier tectonic features related to the accretion of the Arabian Shield [Moore

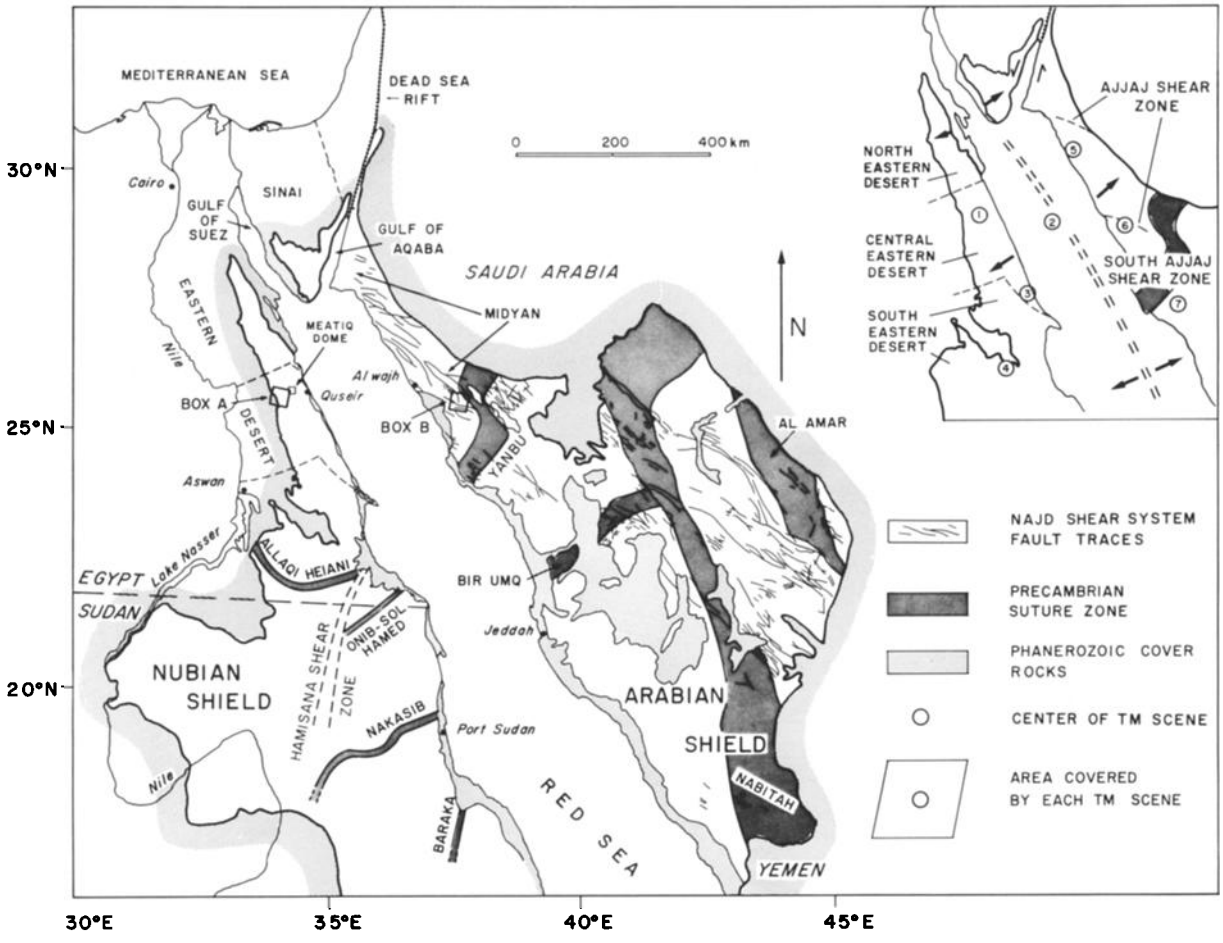

Fig. 1. Place map showing location of the study areas in the Eastern Desert, Egypt and Midyan region, and Saudi Arabia within the Arabian-Nubian Shield. Also shown are inferred boundaries between north Eastern Desert, central Eastern Desert, and south Eastern Desert from Stern and Hedge [1985]; the Ajjaj Shear Zone from Davies [1984]; distribution of suture zones and microplates from Stoeser and Camp [1985] and Kröner et al. [1987]; and outcrop traces of major faults of the Najd System in the Arabian Shield from Moore [1979]. In the upper right corner is a sketch map showing the relative directions of movement for the Arabian and Nubian Shield along the Gulfs of Aqaba and Suez due to opening of the Red Sea [from Garfunkel, 1981]. Full-resolution images for areas outlined by boxes A and B are shown in Figures 3a and 3b, respectively. Locations of the centers of TM scenes used are numbered from 1 to 7. Scene 1 identification number (ID) 5015707420, path 174, row 42, latitude 26.01°N, longitude 33.81°E, date August 5, 1984, sun elevation 58° above horizon, and sun azimuth 100° clockwise from north. Scene 2, ID 5015007360, path 173, row 43, latitude 24.559°N, longitude 35.036°E, date July 29, 1984, sun elevation 59°, and sun azimuth 94°. Scene 3, ID 5015007350, path 173, row 42, latitude 26.008°N, longitude 35.392°E, date July 29, 1984, sun elevation 59°, sun azimuth 97.0°. Scene 4, ID 5015007363, path 173, row 44, latitude 23.125°N, longitude 34.689°E, date July 29, 1984, sun elevation 59°, and sun azimuth 92.0°. Scene 5, ID 5016607355, path 173, row 41, latitude 27.451°N, longitude 35.675°E, date August 14, 1984, sun elevation 57°, sun azimuth 107°. Scene 6, ID 5012707285, path 172, row 42, latitude 25.995°N, longitude 37.011°E, date July 6, 1984, sun elevation 60°, sun azimuth 89°. Scene 7, ID 5008807223, path 171, row 43, latitude 24.548°N, longitude 38.194°E, date May 28 1984, sun elevation 61°, sun azimuth 89°.

and Al-Shanti, 1980; Davies, 1984]. Displacement associated with the NSS was accommodated through ductile stretching and shortening, arcuate folding, and brittle left-lateral faulting [Davies, 1984]. Ductile deformation is commonly more pronounced along anastomosing shear zones of variable lengths and widths. Davies [1984] documented up to 300% stretching deformation along a ductile shear zone over

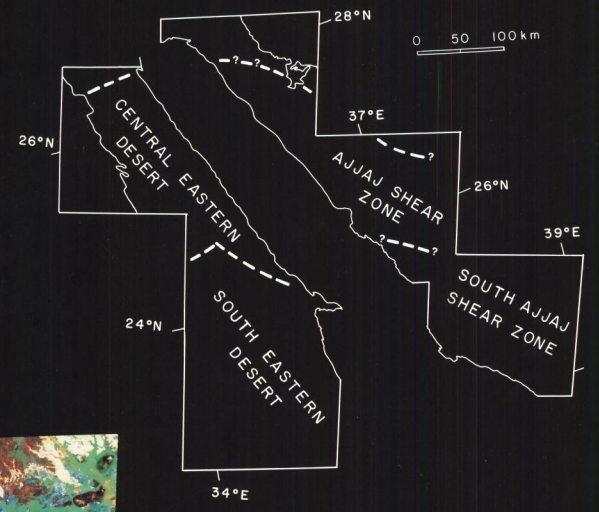

BLUE

BRIGHT IN BAND - 5/4 x 3/4 IMAGE
HIGH IN IRON - BEARING
ALUMINOSILICATE PHASES

GREEN

BRIGHT IN BAND - 5/1 IMAGE
LOW IN SPECTRALLY OPAQUE
PHASES

RED

BRIGHT IN BAND - 5/7 IMAGE
HIGH IN HYDROXYL - OR
CARBONATE BEARING PHASES

0 50 100km

Plate 1a. A color composite image of seven TM scenes in space oblique Mercator projection. TM band 5/4 x 3/4 image is assigned the blue component, band 5/1 the green component, and band 5/7 the red component. The opening of the Red Sea has been accounted for as discussed in the text.

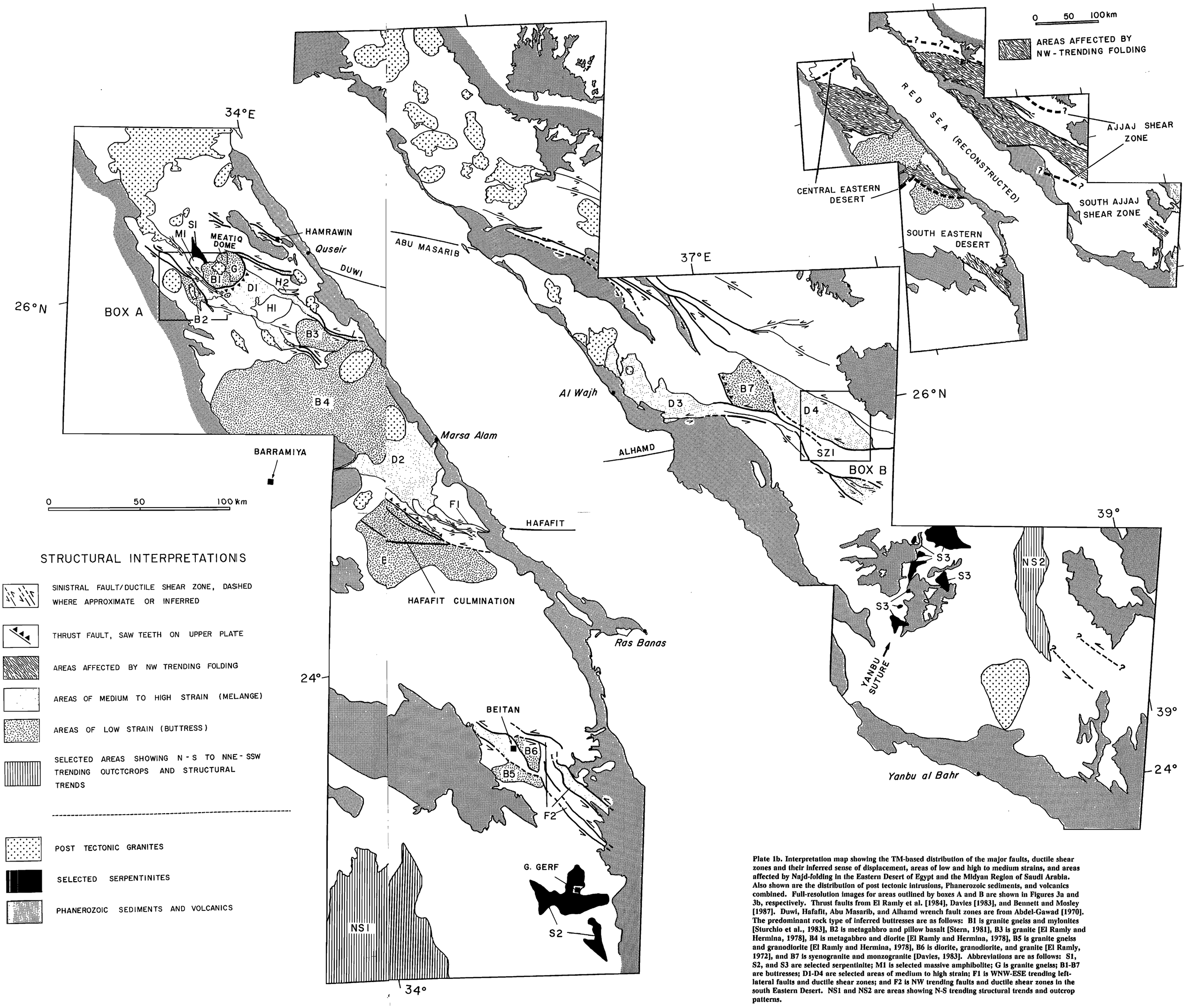

Plate 1b. Interpretation map showing the TM-based distribution of the major faults, ductile shear zones and their inferred sense of displacement, areas of low and high to medium strains, and areas affected by Najd-folding in the Eastern Desert of Egypt and the Midyan Region of Saudi Arabia. Also shown are the distribution of post tectonic intrusions, Phanerozoic sediments, and volcanics combined. Full-resolution images for areas outlined by boxes A and B are shown in Figures 3a and 3b, respectively. Thrust faults from El Ramly et al. [1984], Davies [1983], and Bennett and Mosley [1987]. Duwi, Hafafit, Abu Masarib, and Alhamd wrench fault zones are from Abdel-Gawad [1970]. The predominant rock type of inferred buttresses are as follows: B1 is granite gneiss and mylonites [Sturchio et al., 1983], B2 is metagabbro and pillow basalt [Stern, 1981], B3 is granite [El Ramly and Hermina, 1978], B4 is metagabbro and diorite [El Ramly and Hermina, 1978], B5 is granite gneiss and granodiorite [El Ramly and Hermina, 1978], B6 is diorite, granodiorite, and granite [El Ramly, 1972], and B7 is syenogranite and monzogranite [Davies, 1983]. Abbreviations are as follows: S1, S2, and S3 are selected serpentinite; M1 is selected massive amphibolite; G is granite gneiss; B1-B7 are buttresses; D1-D4 are selected areas of medium to high strain; F1 is WNW-ESE trending left-lateral faults and ductile shear zones; and F2 is NW trending faults and ductile shear zones in the south Eastern Desert. NS1 and NS2 are areas showing N-S trending structural trends and outcrop patterns.

100 km in strike and 20 km in width within the Ajjaj Shear Zone of the Midyan region (Figure 1).

Moore [1979], Abuzied [1984], and Stern [1985] proposed that the NSS projects into the Eastern Desert of Egypt. However, deformation in the Eastern Desert is commonly attributed to obduction-accretion tectonics involving island arcs [e.g., Shackleton et al., 1980; Ries et al., 1983; El Ramly et al., 1984]. The main objective of this paper is to demonstrate through integration of field and Landsat data that structural patterns in part of the Eastern Desert, specifically the central Eastern Desert, are similar to structural patterns within the NSS in Saudi Arabia and to suggest that Najd-related deformation caused many of the structures seen in the central Eastern Desert.

Our approach is to generate Landsat products that emphasize the lithologic and structural characteristics of the NSS near its termination at the Red Sea coast and over its postulated extension in the Eastern Desert. We then characterize structural patterns for areas in the Midyan region where Najd-related deformation has occurred and determine if similar structures can be found in the Eastern Desert. Field observations are used to check inferences drawn from analysis of the Landsat data.

2. DIGITAL LANDSAT THEMATIC MAPPER MOSAICS

The standard Landsat thematic mapper (TM) scene consists of seven images, each 185 by 185 km, registered to one another in a space oblique Mercator projection. Six images are acquired with broadband passes in the 0.4-2.34 μm wavelength region, and one in the thermal infrared (10.4-12.5 μm). Visible and reflected infrared image elements are 30 m across. In this study the visible and reflected infrared data for seven digital scenes are used, covering most of the Midyan region in northern Saudi Arabia and much of the Eastern Desert of Egypt (Figure 1). Data processing involved two stages: (1) processing to emphasize lithologic variations, and (2) processing to correct for the spatial displacement resulting from the opening of the Red Sea.

2.1. Processing to Emphasize Lithologic Information

The procedures used were those applied by Sultan et al. [1986, 1987] in the Eastern Desert. Data for each scene were first converted to brightness values in proportion to bidirectional reflectance, using nominal gain and offset parameters associated with ancillary data files for each scene. Differences in absolute brightness of up to approximately 15% were noticed between adjacent scenes where they overlapped. These variations are due to a combination of variations in extent of atmospheric scattering and absorption and to calibration drift not accounted for in the gain, offset data. Thus the data were normalized to the reflectance of the scene with the least amount of scattering and absorption. That scene was identified on the basis of the lowest overall spectral reflectance over deep water of the Red Sea. Reflectance values were selected for a number of control points in areas of overlap between the control scene and the adjacent scenes. The reflectances for each band in the adjacent scenes were then recomputed to match those of the control scene, using a linear brightness transformation derived from the control point data. The calibrated scenes were then used as control scenes to calibrate other scenes. Scenes with overall reflectance for deep waters similar to the control scene (within 3%) were not altered.

Reflectance ratios have been found to suppress spectral variations due to topography and grain size differences [Rowan et al., 1974; Abrams et al., 1977]. Certain TM band ratios also maximize discrimination of rock types found in the Eastern Desert [Sultan et al., 1986, 1987]. Specifically, Sultan and coworkers found that (1) increasing amounts of spectrally opaque phases with low, flat spectral reflectances (e.g., magnetite, ilmenite, and chromite) decreases the ratio of band 5 (1.55-1.75 μm) to band 1 (0.45-0.52 μm); (2) increasing amounts of hydroxyl-bearing or carbonate minerals (e.g., serpentine and calcite) with vibrational absorptions in TM band 7 wavelength region (2.08-2.35 μm) increases the ratio of band 5 to band 7; and (3) increasing amounts of Fe-bearing aluminosilicates (e.g., hornblende) that absorb in the band 4 wavelength region (0.76-0.9 μm) increases the product of the following two TM ratios: band 5 to band 4 and band 3 (0.63-0.69 μm) to band 4.

The reflectance ratio data were integrated into one color digital mosaic for the seven scenes (Plate 1a) and an interpretation map was produced (Plate 1b). The mosaic shows data presented at an approximate scale of 1:1,000,000 and reduced in resolution by approximately a factor of 2. In generating the interpretation map we used full-resolution hard copy images generated at a scale of 1:150,000.

In Plate 1a the 5/4 x 3/4 image is assigned the blue component, the 5/1 image the green component, and the 5/7 image the red component. Serpentinites with a high abundance of hydroxyl- and/or carbonate-bearing minerals, opaque phases, and a low content of Fe-bearing aluminosilicates appear pure red. For example, the Gebel El Rubshi serpentinites (S1 on Plate 1b) have approximately 10% by volume magnetite, chromite, ilmenite, and other opaque phases and 90% by volume serpentine minerals, talc, chlorite, and carbonate. Serpentinites surrounding Gebel Gerf in the south Eastern Desert and within the NE trending Yanbu suture zone in the Arabian Shield are also red (S2 and S3 on Plate 1b). Granitic rocks with low abundance of opaque phases, hydroxyl-bearing phases, and Fe-bearing aluminosilicates appear green. For example, the granite gneiss in the Meatiq dome area (G in Plate 1b), has approximately 5% by volume amphiboles and less than 1% by volume magnetite. Similarly, post tectonic granites show as green outcrops. These intrusions are outlined in Plate 1b. Mafic rocks that are generally rich in Fe-bearing aluminosilicates and spectrally opaque phases will have a blue color since the ratio 5/4 x 3/4 will be high [Sultan et al., 1987]. For example, massive

amphibolites (M1 in Plate 1b) to the NW of the Meatiq dome have approximately 60% by volume amphiboles and 3% by volume magnetite and appear blue.

2.2. Processing to Remove the Spatial Displacement Associated With the Red Sea Rifting

The opening of the Red Sea at 25 Ma [Cochran, 1983] was associated with left-lateral displacement along the Gulf of Aqaba and the Dead Sea Rift and extension in the Gulf of Suez. The directions of displacement caused by the Red Sea rifting are shown in the upper right corner of Figure 1. The extension in the Gulf of Suez is approximately 30 km [Steckler, 1985], and left-lateral motion along the Gulf of Aqaba is approximately 110 km [Freund et al., 1970]. These estimates were based primarily on the onshore geology and were used to restore Africa and the Arabian Peninsula to their prerifting positions [Freund, 1970; Girdler and Darracott, 1972; Cochran, 1981]. These reconstructions predict that continental crust underlies most of the current Red Sea rift and that the restored Red Sea coasts are widely separated (approximately 80-100 km apart). Alternatively, studies based on seismic refraction data [Bohannon, 1986a, b], magnetic data [Girdler and Styles, 1974], plate kinematics [McKenzie et al., 1970], and Gemini and Apollo photographs [Abdel-Gawad, 1970] suggest that oceanic crust underlies most of the current Red Sea rift and that the separation between the restored Red Sea coasts is negligible.

We used the conservative estimates of the displacement magnitudes and directions outlined above to translate the TM scenes for the Eastern Desert and the Midyan region to their approximate prerift relative positions (Plates 1a and 1b). Examination of Plates 1a and 1b show that the northwesterly extension of the Ajjaj Shear Zone region would be generally into the central Eastern Desert. Note that the Red Sea shores in this reconstruction are approximately 80-100 km apart. If we were to increase the closure of the Red Sea so that the shores are approximately 20-40 km apart, the Duwi and Hafafit wrench fault zones in the Eastern Desert would align with the Abu Masarib and Alhamd wrench fault zones in Saudi Arabia (Plates 1a and 1b), respectively, as predicted by Abdel-Gawad [1970]. Given the limited number of crosscutting features in the study area, and the uncertainty in their strike in between the Red Sea coasts, we are unable to resolve these controversial issues regarding the nature of the crust underlying the Red Sea and the amount of separation between the restored Red Sea coasts. However, even if we used the conservative estimates, the central Eastern Desert will still mark the extension of the Najd Shear System into the Eastern Desert. Thus we conclude that the central Eastern Desert is the most likely area to search for structures similar in style to those found in the Ajjaj Shear Zone.

3. STRUCTURAL CONSTRAINTS ON THE EXTENSION OF THE NAJD SYSTEM INTO THE EASTERN DESERT FROM TM-BASED LITHOLOGIC MAPS, FIELD OBSERVATIONS, AND AVAILABLE GEOLOGIC MAPS

The NSS trends NW-SE and enters the Red Sea rift as the Ajjaj Shear Zone between 26° and 27°45'N latitude; the most conspicuous trend intersects the Red Sea coast at 27°20'N latitude [Brown, 1970]. The Ajjaj Shear Zone has an exposed strike length of at least 200 km and a width of approximately 100 km (Figure 1) [Davies, 1984].

Inspection of Plate 1a shows that the outcrop patterns of the the Ajjaj Shear Zone and the central Eastern Desert are similar, as are those in the region south of the Ajjaj Shear Zone and in the south Eastern Desert. The Ajjaj Shear Zone and central Eastern Desert outcrops are predominantly NW elongated and show fine-scale lithological diversity. In contrast, outcrop patterns in the region south of the Ajjaj Shear Zone and the south Eastern Desert are relatively equant, with lithologic variability occurring on a large scale. For example, serpentinites in the central Eastern Desert show a different pattern from those in the south Eastern Desert (red outcrops in Plate 1a). On the basis of the Red Sea reconstruction (section 2.2) and examination of outcrop patterns discussed above, we conclude that there is strong evidence that the Ajjaj Shear Zone extends into the central Eastern Desert.

We developed criteria for identifying Najd-related folding, sinistral faults and ductile shear zones, and areas of high and low strain from TM data covering the Midyan region in Saudi Arabia. These structural elements are shown in the interpretation map (Plate 1b). We then searched for similar features in the central Eastern Desert to test the hypothesis that NSS projects into the central Eastern Desert. Field data in Saudi Arabia and the Eastern Desert were used to test our interpretations. We also used single-band TM images in conjunction with the TM color mosaic when additional topographic information was needed to help delineate particular structural elements because the mosaic (Plate 1a) de-emphasizes spectral variations related to topographic relief. Areas to the north of the Ajjaj Shear Zone and the central Eastern Desert do not exhibit major NW-SE trending structures characteristic of the Najd Shear System in Arabia [Brown, 1970; Stern, 1985], and thus these areas were not examined.

3.1. Areas Affected by NW trending Folding

In the Midyan region the areas occupied by the NSS are characterized by a general NW trending outcrop pattern predominantly controlled by Najd-related folding. This conclusion is based on comparison of the spatial congruency between NW trending outcrops in Plate 1a and areas occupied by Najd-related folds extracted from geologic maps (Figure 2). Similar outcrop patterns and fold traces have been reported in

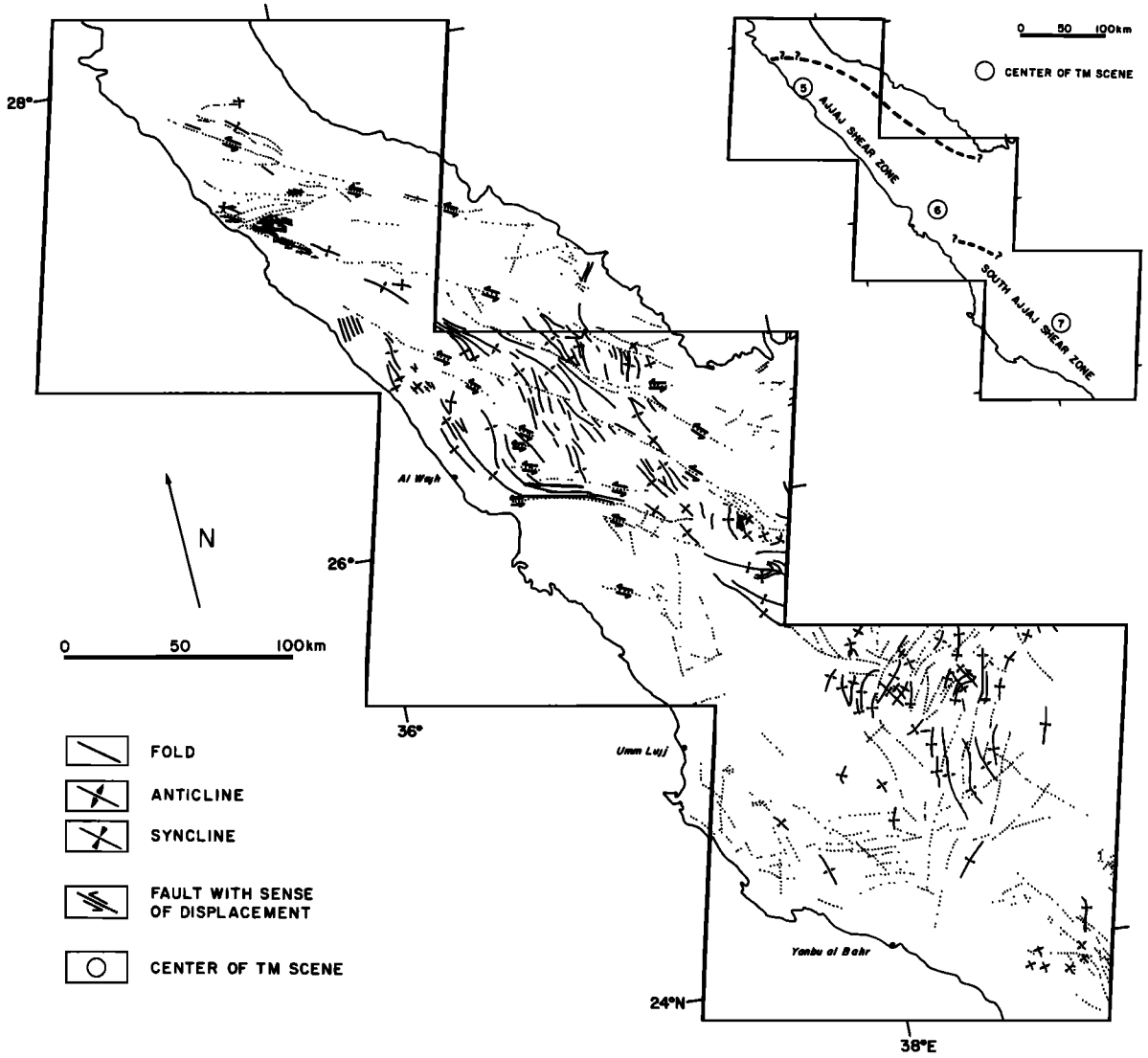

Fig. 2. Structural sketch map showing the major faults and folds for the area occupied by the examined TM scenes and surrounding areas in Saudi Arabia. Map compiled from Smith [1979], Dhellemmes and Delfour [1980], Clark [1981], Kemp [1981], Pellaton [1979, 1981, 1982a, b] Davies [1980, 1983], Johnson [1983], and Davies and Grainger [1985].

many other areas occupied by the NSS elsewhere in the Arabian Shield [Delfour, 1979; Letalenet, 1979; Moore, 1979; Kemp et al., 1982]. The identification of individual folds from TM images is hindered by (1) the compositional similarities of folded units, and/or (2) the tight nature of many Najd-related folds. Both factors render the identification of closures in folded units difficult. Thus no attempt is made to map individual folds. Instead, we mapped domains affected by NW trending folding (Plate 1b). In the south Ajjaj Shear Zone the prominent trend is N-S to NNE-SSW; the Najd NW trend is not conspicuous (Plates 1a and 1b and Figure 2). Examples of these outcrops are labeled NS2 on Plate 1b. These N-S to NNE-SSW trends are controlled by folds, as indicated by examination of detailed geologic maps [Pellaton, 1979; Kemp, 1981].

Similar structural observations to those observed in the Ajjaj Shear Zone and to the south of the Ajjaj Shear Zone are reported from the central Eastern Desert and south Eastern Desert, respectively. Locally, NW trending outcrop patterns in the central Eastern Desert have been shown to be controlled by NW trending open to tight folds [El Shazly, 1964; Abdel-Khalek, 1980; Stern, 1981; Abuzied,1984; Greene, 1984; Greiling

et al., 1984]. In the south Eastern Desert, N-S to NNE-SSW trending structural trends and outcrop patterns are observed (e.g., areas labeled NS1 on Plate 1b) and NW trending outcrops are absent except for a minor NW trending zone (Plate 1a) labeled F2 in Plate 1b. Outcrop patterns within parts (wadi Beitan area, Plate 1b) of this minor zone are controlled by NW trending folds [Abdel-Khalek, 1980].

We mapped areas affected by NW trending folding in the Midyan region and the Eastern Desert, and the results are shown in the upper right corner of Plate 1b. These areas are characterized by NW trending outcrop patterns and structural trends as seen in TM data. Note that both the Ajjaj Shear Zone and the central Eastern Desert show NW trending folds.

3.2. Strike-Slip Faults and Ductile Shear Zones

Numerous left-lateral faults and ductile shear zones are reported along the Ajjaj Shear Zone [Davies, 1984]. By examining full-resolution TM images over these faults and shear zones, we developed criteria to identify Najd-related faults and shear zones and to determine the nature (brittle versus ductile) of deformation and sense of displacement. Figures 3a and 3b are full-resolution images for the areas covered by boxes A and B, respectively, in Figure 1 and Plate 1b. These figures illustrate criteria for identification of Najd-related faults and shear zones from TM data. Figures 3c and 3d are TM-based interpretation maps for Figures 3a and 3b, respectively, drawn using three criteria defined in ensuing paragraphs.

Criteria 1 is the presence of NW trending lithologic discontinuities that are tens of meters (faults) to hundreds of meters (shear zones) wide. Both faults and shear zones show left-lateral offsets. The sense of displacement was commonly determined from the changes in directions of structural trends and outcrop patterns of distinctive lithologies, as they approach the inferred fault or ductile shear zone trace and less commonly determined by observing displacement of distinctive lithologies across the discontinuity. Figures 3b and 3d show N-S trending outcrop patterns and structural trends subtended between a shear zone to the south and strike-slip faults to the north that change their orientation to align with the bounding NW trending faults and shear zones, developing sigmoidal patterns. The sigmoidal patterns indicate left-lateral displacement along the bounding faults and shear zone. The inferred left-lateral faults and shear zone were confirmed through comparison with available geologic maps [Kemp, 1981; Pellaton, 1982b; Davies, 1983].

Criteria 2 is the presence of stretched outcrops, especially serpentinites, within the inferred shear zones and along some of the fault traces, implying that deformation was partly accommodated through ductile deformation. The inferred ductile nature of the shear zone shown in Figure 3b and outlined in Figure 3d was confirmed through the following field observations along the shear zone and its extension some 30 km to the north: (1) ductile stretching strains of up to 300% of the original dimension, (2) subhorizontal linear penetrative fabrics, and (3) congruency between axial surfaces of the folds, slaty cleavage, penetrative linear fabrics, and the walls of the shear zone [Kemp, 1981; Davies, 1983].

Criteria 3 is the presence of subparallel topographic ridges within the inferred ductile shear zones, seen in individual band TM images. These ridges are probably related to differential weathering of compositionally different, subparallel lithologic units within the shear zones. For example, the band 3 image (Figure 4) for the area covered by Figures 3b and 3d shows subparallel ridges within the ductile shear zone outlined in Figure 3d.

Similar structural observations to those described above can be found in the central Eastern Desert. For example, Figures 3a and 3c show the following:

1. Outcrop patterns for rock units within the shear zone are elongated as compared to lithologically similar rocks outside the zone. For example, note differences in outcrop patterns of serpentinites and amphibolites within as opposed to outside the shear zone.
2. Trails of serpentinites are observed along fault traces. For example, numerous stretched out serpentinite outcrops along faults A-A' and B-B' (Figure 3c). Faults have been observed elsewhere to be preferentially localized along serpentinite outcrops since these rocks accommodate movement efficiently and at low temperatures through ductile deformation [Raleigh and Paterson, 1965].
3. Outcrop patterns and structural trends change their orientation to align with inferred shear zones and fault traces. An example of this is the N-S trending serpentinite outcrops surrounding the Bir Fawakhir granite that change their orientation to align with the NW trending shear zone.

The inferred ductile style of deformation for the shear zones seen in Figure 3c was confirmed through our reconnaissance field work in the Fawakhir area, as well as field work by Ries et al. [1983] and Bennet and Mosley [1987]. The following field observations from these areas are pertinent to confirming a ductile style of deformation: (1) NW trending subhorizontal mineral and stretching lineations, (2) NW trending foliation, and (3) congruency between axial traces of folds, penetrative planar and linear fabrics described above, and the inferred walls of the shear zone.

Using some or all of the above mentioned criteria, we mapped the major faults and shear zones (Plate 1b). Smaller and less obvious ones are not shown.

3.3. Areas of Medium to High Strain (Melanges?)

Examination of Plate 1a shows that in the Ajjaj Shear Zone there are areas that show considerable fine-scale heterogeneity on the outcrop scale (tens to hundreds of meters). Some areas that show this character distinctly are located between the Najd-related faults and the ductile shear zone shown in Figures 3b and 3d. The spatial correlation with shear zones and

faults suggests a causal relationship. For example, these highly complex areas might lie within ductile shear zones, at their terminations, or within adjacent faults and/or shear zones.

Similar areas were identified in the Eastern Desert (Plates 1a and 1b). Two examples are the areas located to the south of the Meatiq dome (D1 in Plate 1b) and the wadi Ghadir and surrounding areas (D2 on Plate 1b). On the basis of our field observations and those of El-Sharkawy and El-Bayoumi [1979], Ries et al. [1983], El Bayoumi [1984], and Habib et al. [1985] the fine-scale heterogeneity seen in TM data is caused by lithological heterogeneity. Highly dismembered ophiolitic rock associations are found in a melange composed predominantly of fragmented, serpentinized ultramafic rocks, sheeted dikes, pillow basalt, layered and massive gabbro, and sedimentary rocks of oceanic facies. Individual lithologically distinct fragments average tens of meter in size and range from cobble to mountain size. All lithologic contacts are tectonic and not stratigraphic. We did not observe a pervasive matrix in between the rock fragments, as described by the above mentioned workers. For example, in the wadi Ghadir area, contacts between lithologic units are sharp. Only locally, along highly tectonized shear zones, do competent rocks appear to be embedded in a finer-grained matrix. This observation is important to the tectonic analysis discussed in the next section.

We have mapped areas of extensive deformation based on the following TM-based characteristics and field observations: (1) fine-scale heterogeneity on the scale of tens to hundreds of meters seen on TM data, and (2) similar fine-scale lithologic heterogeneities seen in outcrop or reported in literature. Results are shown in Plate 1b.

3.4. Areas of Low Strain (Buttresses)

Plate 1a shows that the shear zones and faults have a NW trend but abruptly change strike near large bodies of competent rocks such as granite. The NW trending ductile shear zone (SZ1) bifurcates into E-W and N-S trending shear zones around a large granitic body (B7 in Plate 1b). As the ductile shear zones change their orientation, they develop a thrust component that depends on the extent to which the shear zone has changed in strike and dip. Thus thrust faults frequently occur at the intersection of shear zones and large competent bodies. The B7 granite in Plate 1a is structurally concordant with the surroundings, indicating a pretectonic or syntectonic mode of emplacement. Davies [1983] describes this pluton and others belonging to the Marabit Complex found within the Najd-related ductile shear zones, as deformed lensoid diapirs, confirming the mode of emplacement inferred from TM products.

Large rock bodies such as B7, showing some or all of the following criteria from TM and field data, are mapped as buttresses in Plate 1b and are labeled with "B" designation:

Criteria 1 is the presence of large rock bodies that are composed predominantly of competent rock units such as granite, diorite, and gabbro. Competent rocks of granitic composition can be readily mapped from TM images (refer to section 2.1), but more mafic types such as gabbros cannot be differentiated from chemically similar, yet mineralogically different, incompetent rocks such as greenschists. Thus additional information regarding the rock type of the inferred buttresses was also extracted from available geologic maps (refer to caption of Plate 1b).

Criteria 2 is the presence of rock bodies that deflect the orientation of strike-slip faults and ductile shear zones as they approach the inferred buttresses, giving rise to thrust faults. The identification of thrust faults from TM images is not as straightforward as strike-slip faults and shear zones. Unlike strike-slip fault traces that generally appear as long linear features on TM images, thrust fault traces are highly irregular, rendering their identification from TM data difficult. Thus thrust faults shown on Plate 1b are based on published geologic maps.

Criteria 3 is the presence of conformable boundaries between the inferred buttresses and their surroundings. This criterion allows separation of buttresses from post tectonic intrusions that crosscut their surroundings (e.g., granite intrusion surrounding G. Um Had in Figures 3a and 3c).

Criteria 4 is the presence of rock bodies that possess highly sheared, commonly mylonitized margins, with the intensity of deformation decreasing away from the margins toward the interior of the body seen in the field.

We have mapped a number of areas in the Eastern Desert that show the characteristics outlined above. For example, note that the buttress marked B5 (Plate 1b) is composed primarily of granites and granodiorites. WNW-ESE trending strike-slip faults and the ductile shear zone (labeled F1 in Plate 1b) intersect the NE margin of the buttress, an area known as the Hafafit Culmination [El Ramly et al., 1984]. At the intersection we observe the following: (1) the faults and shear zones are reoriented along a NW trend and develop a thrust component (Plate 1b), (2) subhorizontal NW trending mineral-stretching lineations [Greiling, 1987; Greiling et al., 1988] and subvertical foliations [El Ramly et al., 1984; Greiling et al., 1984] predominate. Bennett and Mosley [1987] explain the above mentioned features in the Hafafit Culmination and other structurally similar areas (e.g., Meatiq dome), as resulting from Najd-related thrusting in a duplex system.

4. DISCUSSION AND IMPLICATIONS OF THE EXTENSION OF THE NAJD SYSTEM INTO THE EASTERN DESERT

The NSS was first recognized some 20 years ago in the central and southern parts of the Arabian Shield. For example, Brown [1972] documented a cumulative sinistral displacement of 240 km through correlation of displaced N-S trending ophiolitic belts (Figure 1). Stern

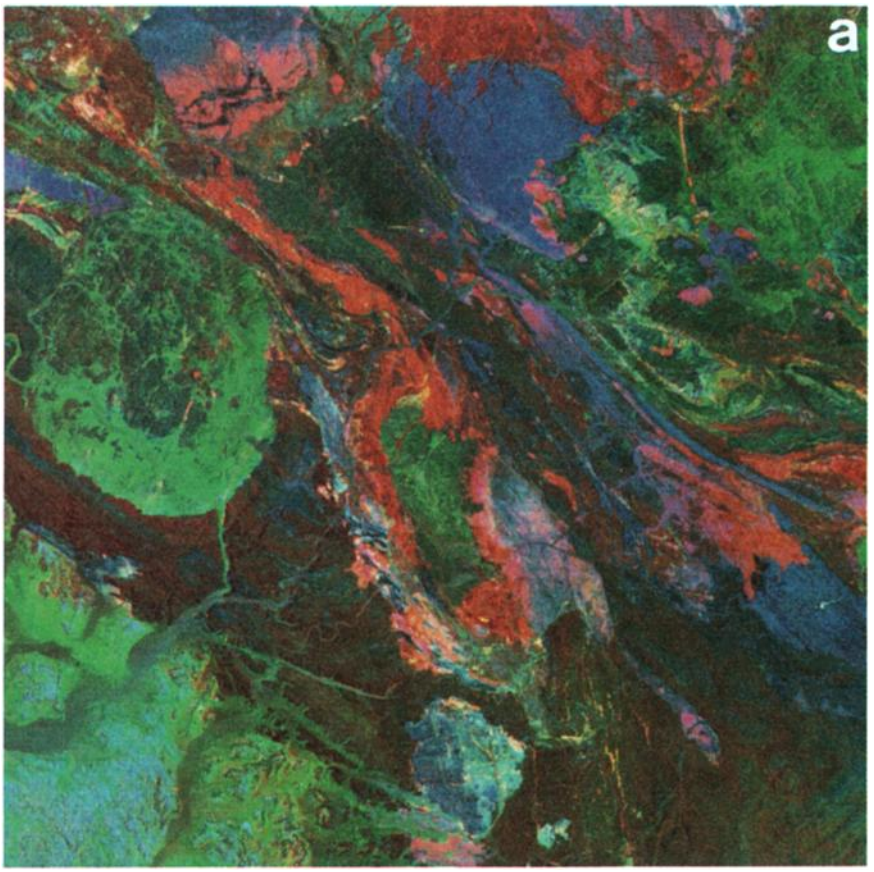
a


b

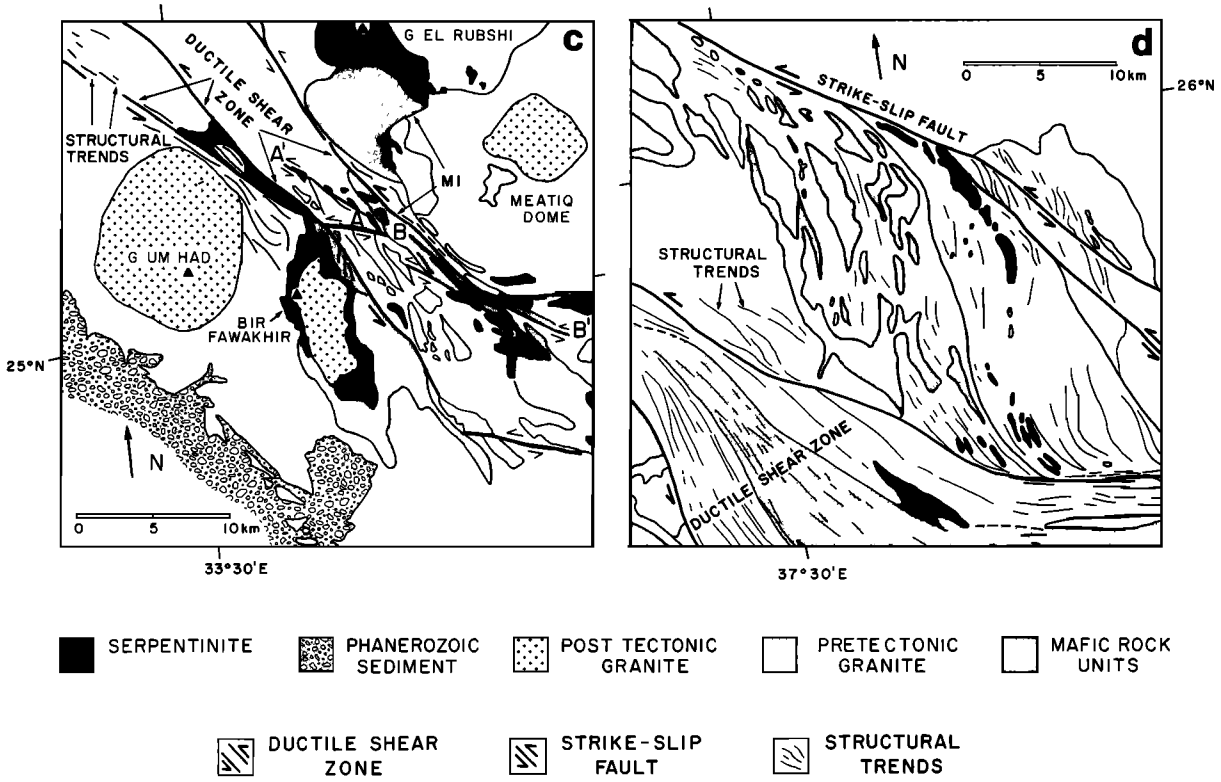

Fig. 3 (a) and (b) Full-resolution images for the area covered by boxes A and B in Plate 1b, respectively. Reproduced by permission of Earth Observation Satellite Company, Lanham, Maryland. (c) and (d) Interpretation maps showing Najd-related faults and shear zones and their inferred sense of displacement for Figures 3a and 3b, respectively. M1 denotes selected amphibolite outcrops within and outside the ductile shear zone. Selected outcrops were outlined within and outside the shear zones to demonstrate the stretching and the dismembering of outcrops in areas of medium to high strain.

[1985] argued that the dimensions and orientations of the NSS is better understood in central and southern Saudi Arabia, as compared to the areas in the north (Midyan region and Eastern Desert). He cited the following reasons: (1) the abundance of granitic bodies intruded through the Najd lines of weakness in the north, and (2) the predominance of ductile deformation in the north as opposed to brittle deformation in the south. In addition, there are no obvious displaced units (e.g., linear ophiolitic belts crosscutting the NSS in central Saudi Arabia) in the north. However, it became clear that the Ajjaj Shear Zone structures are Najd-related, given the continuity of structural patterns with Najd-related features located to the SE and the dominance of left-lateral displacements in the Ajjaj Shear Zone.

Following the recognition of the NSS in Saudi Arabia, Moore [1979] speculated that the NW termination of the NSS should be in the Eastern Desert of Egypt. The probable extension of the NSS into the Eastern Desert was first illustrated locally by Abuzied [1984], and its regional extent was first suggested by Stern [1985]. Abuzied documented deformation characteristic of the NSS in the Hamrawin area, approximately 10 km NW of Quseir (Figure 1). Stern [1985] reinterpreted the observed NW trend commonly reported in the central Eastern Desert for fault traces, pencil lineations, and pebble and mineral stretching lineations, as resulting from movement along a segment of the NSS and not due to thrusting, as had previously been suggested. However, the extension of the NSS into Egypt has remained unsubstantiated in the absence of published detailed structural maps on a regional scale.

Using TM data, we have mapped numerous NW trending left-lateral faults and ductile shear zones in the Ajjaj Shear Zone and the central Eastern Desert (Plate 1b). Most of these left-lateral faults and ductile shear zones in the Eastern Desert are not reported in published geologic maps. The presumed absence of such faults and ductile shear zones has led workers to assume the absence of the Najd System in the central Eastern Desert and to relate the tectonic features observed in the Eastern Desert solely to the accretion of the Nubian Shield.

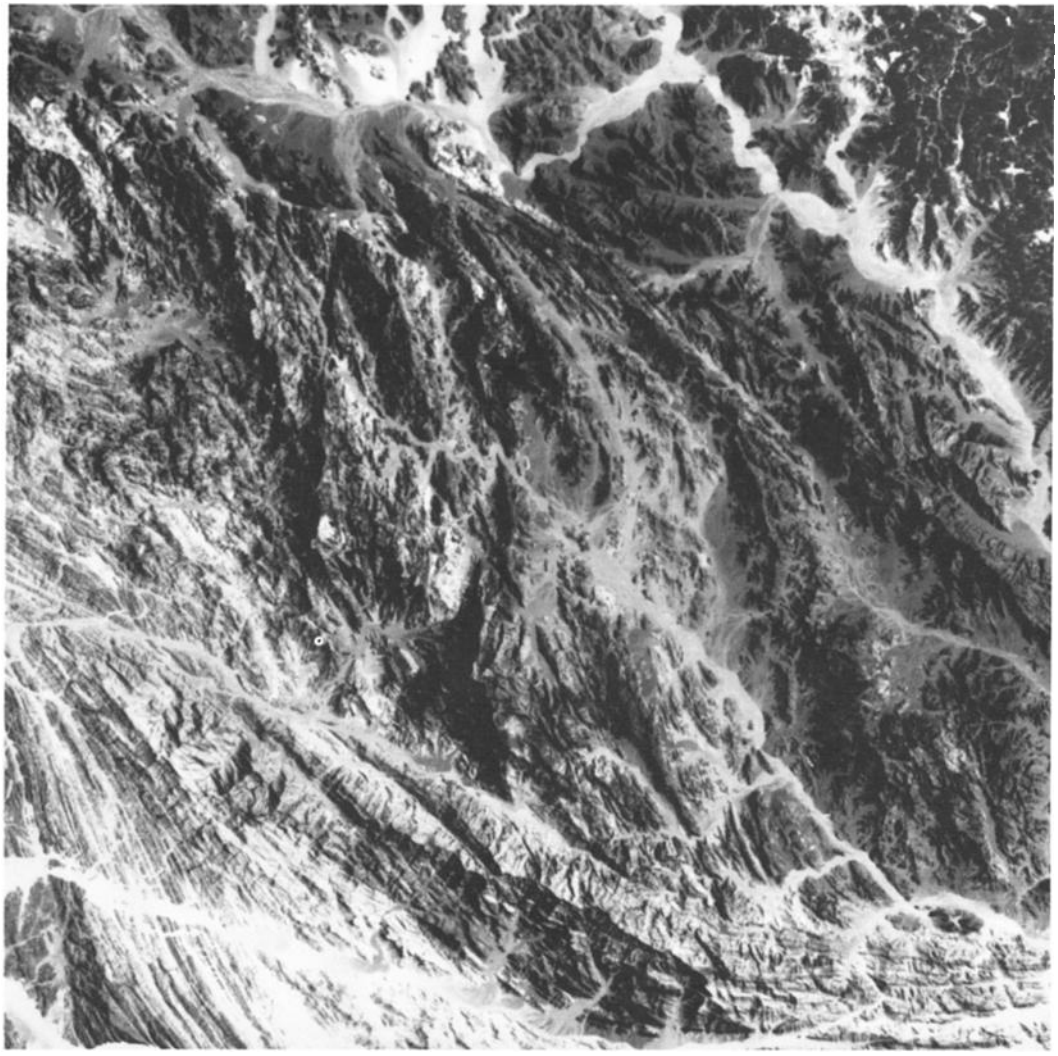

Fig. 4. Landsat TM band 3 image for the area covered by Figures 3b and 3d showing subparallel topographic ridges within the ductile shear zone outlined in Figure 3d. Reproduced by permission of Earth Observation Satellite Company, Lanham, Maryland.

We have demonstrated that the Ajjaj Shear Zone and the central Eastern Desert share the following field and TM-based characteristics: (1) NW trending folds, (2) thrust faults and local modifications in penetrative deformation developing as strike-slip faults and ductile shear zones approach buttresses, (3) penetrative subhorizontal NW mineral lineations, (4) variably dipping NW trending foliations, and (5) predominance of tectonic contacts. In the Ajjaj Shear Zone these features have been interpreted to be a consequence of NSS deformation. However, in the central Eastern Desert these features have previously been assigned other origins. For example, the thrust faults reported to the NE of the B5 buttress are presumed to be related to an overthrusting event during continent/arc collision [El Ramly et al., 1984]. The open NW trending folds in the central Eastern Desert have been thought to be indicative of a NE-SW directed compressional event [Sturchio et al., 1983]. The subhorizontal NW trending mineral lineations commonly reported in the central Eastern Desert (and rarely reported in the south Eastern Desert) have been thought to indicate the direction of tectonic transport of nappes [Ries et al., 1983]. Local modifications in the general NW trending penetrative deformation around large domains composed of competent rock types remain unaccounted for in many areas, for example, the E-W trending cleavage in the Barramyia area [Shukri and Lotfi, 1955]. We propose that the NW trending ductile shear zone and left-lateral faults running parallel to the Hahafit Culmination

change their orientation to align with the E-W trending buttress (labeled B4 on Plate 1b). This body is composed predominantly of metagabbro, diorite, and epidiorite [El Ramly, 1972; El Ramly and Hermina, 1978].

The predominance of highly deformed rocks showing ophiolitic affinities in the central Eastern Desert has been interpreted as an extensive ophiolitic melange [Ries et al., 1983; Shackleton et al., 1980]. It is widely thought that the ophiolitic melange in the Eastern Desert is partly trench and partly tectonic melange, perhaps related to the Sol Hamed-Onib suture some 300-500 km to the south [Ries et al., 1983](Figure 1). Shackleton et al. [1980] concluded that the ophiolites are allochthonous, transported by gravity sliding in a trench, followed by thrusting through nappe emplacement.

We favor the hypothesis that Najd-related deformation is responsible for the dismemberment of the ophiolitic sequence and production of the melange for the following reasons:

1. Extensive melanges are absent in the Midyan region, despite the continuation of the Sol Hamed-Onib suture in the Midyan region as the Yanbu suture zone (Figure 1 and Plate 1b). If the melanges of the Eastern Desert are related to the Sol Hamed-Onib-Yanbu suture, we would expect a similar melange to be present in the Midyan region.

2. There is a close spatial correlation between the distribution of so-called melanges with the postulated extension of the NSS in the Eastern Desert. The melanges as described earlier are clearly affected by Najd-related NW-SE structures.

3. Melanges of the central Eastern Desert are not typical trench melanges because they lack the pervasive matrix on a regional scale that is typical of such melanges reported elsewhere. Typical melanges are formed of "blocks in a matrix" [Raymond, 1984]. The matrix in melanges in other regions of the world is pervasive; only locally is the matrix missing [e.g., Yilmaz and Maxwell, 1984].

4. Finally, Shackleton et al. [1980] also realized that their model had shortcomings, especially the lack of evidence for extensive tectonic transport that would be required.

NW trending folds, structural trends, left-lateral faults and ductile shear zones, and penetrative planar and linear fabrics are uncommon in the area south of the Ajjaj Shear Zone and in the south Eastern Desert, based on analysis of TM data and published geologic maps. Instead, the dominant tectonic fabric in these areas is N-S to NNE-SSW (Plate 1b). These trends represent the dominant tectonic grain in the Arabian Shield [Brown and Coleman, 1972; Moore, 1979]. Stoeser and Camp [1985] have shown that the suture zones, predating the Najd System, have a N-S to NE-SW trend (Figure 1). These sutures probably control the N-S to NNE-SSW structures discussed above. Modes of emplacement of mafic/ultramafic sequences in the central Eastern Desert and south Eastern Desert are different. In the central Eastern Desert, mafic/ultramafic sequences are all in tectonic contact [Shackleton et al., 1980]. In contrast, mafic/ultramafic sills with intrusive contacts were reported in the south Eastern Desert [Dixon, 1981]. Thus we conclude that records of the accretionary history of the Arabian-Nubian Shield are probably better preserved in the south Ajjaj Shear Zone and the south Eastern Desert compared to the Ajjaj Shear Zone and the central Eastern Desert.

5. SUMMARY

1. A digital color mosaic compiled from seven Landsat thematic mapper scenes was used to delineate characteristic structural features for the NSS in the Midyan region of Saudi Arabia and to search for similar features in the Egyptian Eastern Desert. The digital mosaic was generated using ratios of Landsat thematic mapper bands (5/4 x 3/4, 5/1, and 5/7). These ratios are sensitive to the rock content of Fe-bearing aluminosilicates, spectrally opaque phases, and hydroxyl-bearing or carbonate minerals of the outcrops, respectively. The mosaic covers approximately 130,000 km^2 of late Proterozoic exposures of the Arabian-Nubian Shield and has the Eastern Desert and the Midyan region placed in their approximate pre-Red Sea locations. Approximately 30 km of extension within the Gulf of Suez and 110 km of left-lateral motion along the Gulf of Aqaba were used to define displacement magnitudes and directions for corrections to pre-Red Sea locations.

2. The Ajjaj shear zone that marks the termination of the Najd System against the eastern margin of the Red Sea aligns with the central Eastern Desert, based on analysis of pre-Red Sea locations.

3. We have mapped for the first time left-lateral faults and ductile shear zones in the Eastern Desert characteristic of the Najd System in Saudi Arabia. The presumed absence of such features has led workers to assume that the NSS is absent in the Eastern Desert and to relate deformation in the Eastern Desert entirely to obduction/accretion tectonics.

4. Analyses of Landsat data and field observations show that the Ajjaj Shear Zone and the central Eastern Desert exhibit the following features in common: (1) outcrops that are generally elongate in a NW-SE direction due to folding, with fine-scale lithologic heterogeneity at the outcrop scale due to deformation associated with faulting, (2) NW trending left-lateral faults and ductile shear zones, (3) subhorizontal, NW trending mineral lineations, (4) variably dipping NW trending foliations, with local changes in attitude around competent (e.g., granitic) rocks, and (5) lithologic contacts that are generally tectonic in nature and related to faulting. These features are less common to the north and south of both the Ajjaj Shear Zone and the central Eastern Desert. We propose that these features are largely controlled by Najd deformation and are not the result of obduction/accretion tectonics as currently accepted.

5. We propose that the dismembering of the ophiolitic sequences of the Eastern Desert are related largely to Najd deformation. This hypothesis differs from interpretations that explain the dismembering of the ophiolitic sequences in the Eastern Desert through gravity sliding in a trench and/or thrusting through nappe emplacement accompanying arc/arc or arc/continent collision.

6. Records of the pre-Najd accretionary history of the Eastern Desert are probably better preserved in the south Eastern Desert where the Najd deformation was apparently less pronounced.

7. Geologists involved in the tectonic synthesis of large domains of the lesser known continents such as the Arabian-Nubian Shield are often faced by the absence of (1) detailed geologic maps on a regional scale, (2) reliable databases for geochronologic and geochemical data, and (3) integrated studies between research groups working within particular political boundaries. We have shown that these difficulties can be somewhat alleviated if conventional data sources are combined with lithologic and structural inferences made from spaceborne observations. Implications for similar applications elsewhere are clear.

Acknowledgments. Supported by NASA Geology Program under contracts NASW 4017 and NAGW 1358 to Washington University. We thank J. Alt, R. Bohannon, K. Burke, T. Dixon, G. Green, J. Luhr, R. Lyon, N. Sturchio, and D. Wise for helpful comments and conversations and M. Bassiouni, A. Dardir, G. Naim, M. Francis, I. Shalaby, and M. Youssef for providing logistical support for fieldwork in Egypt. The manuscript, images, and illustrations were prepared at the Earth and Planetary Remote Sensing Laboratory, McDonnell Center for the Space Sciences, Washington University, and the Jet Propulsion Laboratory with help from M. Dale-Bannister, F. Johnson, R. Kieffer, C. Kozlosky, C. Martin, and H. Mortensen.

REFERENCES

Abdel-Gawad, M., Interpretation of satellite photographs of the Red Sea and Gulf of Aden, Philos. Trans. R. Soc. London, Ser. A, 267, 23-40, 1970.

Abdel-Khalek, M.L., Tectonic evolution of the basement rocks in the southern and central Eastern Desert of Egypt, in Evolution and Mineralization of the Arabian-Nubian Shield, vol. 1, edited by A.M.S. Al Shanti, pp. 53-62, Pergamon, Elmsford, N.Y., 1980.

Abrams, M.J., R.P. Ashley, L.C. Rowan, A.F.H. Goetz, and A.B. Kahle, Mapping of hydrothermal alteration in the Cuprite mining district, Nevada, using aircraft scanner images for the spectral region 0.46 to 2.36 μm, Geology, 5, 713-718, 1977.

Abuzied, H.T., Geology of the Wadi Hamrawin Area, Red Sea Hills, Eastern Desert, Egypt, Ph.D. thesis, 206 pp., Univ. of S. C., Columbia, 1984.

Agar, R.A., The Najd fault system revisited; a two-way strike-slip orogen in the Saudi Arabian Shield, J. Struct. Geol., 9, 41-48, 1987.

Bennett, J.D., and P.N. Mosley, Tiered-tectonics and evolution, Eastern Desert and Sinai, Egypt, in Current Research in African Earth Sciences, edited by G. Matheis and H. Schandelmeier, pp. 79-82, Balkema, Rotterdam, Netherlands, 1987.

Bohannon, R.G., How much divergence has occurred between Africa and Arabia as a result of the opening of the Red Sea?, Geology, 14, 510-513, 1986a.

Bohannon, R.G., Tectonic configuration of the western Arabian continental margin, southern Red Sea, Tectonics, 5, 477-499, 1986b.

Brown, G.F., Eastern margin of the Red Sea and the coastal structures in Saudi Arabia, Philos. Trans. R. Soc. London, Ser. A, 267, 75-87, 1970.

Brown, G.F., Tectonic map of the Arabian Peninsula, scale 1:4,000,000, Map Ap-2, Saudi Arabia Dir. Gen. of Miner. Resour., Jiddah, 1972.

Brown, G. F., and R.G. Coleman, The tectonic framework of the Arabian Peninsula, Int. Geol. Congr. Rep. Sess. 24th, 3, 300-305, 1972.

Clark, M.D., Geologic map of the Al Hamra quadrangle, sheet 23C, Kingdom of Saudi Arabia, scale, 1:250,000, Geol. Map GM Saudi Arabia Dep. Minist. Miner. Resour., GM-49A, 28 pp., 1981.

Cochran, J.R., The Gulf of Aden: Structure and evolution of a young ocean basin and continental margin, J. Geophys. Res., 86, 263-288, 1981.

Cochran, J.R., A model for development of Red Sea, Am. Assoc. Pet. Geol. Bull., 67, 41-69, 1983.

Davies, F.B., Reconnaissance geology of the Duba quadrangle, sheet 27/35D, Kingdom of Saudi Arabia, scale 1:100,000, Geol. Map GM Saudi Arabia Dir. Gen. Miner. Resour., GM-57, 23 pp., 1980.

Davies, F.B., Geology of the Al Wajh quadrangle, sheet 26B, Kingdom of Saudi Arabia, Open File Rep. DGMR-OF-03-8, 81 pp., Saudi Arabia Dep. Minist. for Miner. Resour., Jiddah, 1983.

Davies, F.B., Strain analysis of wrench faults and collision tectonics of the Arabian-Nubian Shield, J. Geol., 82, 37-53, 1984.

Davies, F.B., and D.J. Grainger, Geologic map of the Al Muwaylih quadrangle, sheet 27A, Kingdom of Saudi Arabia, scale 1:250,000, Geosc. Map GM Saudi Arabia Dep. Minist. Miner. Resour., GM-82A, 32 pp., 1985.

Delfour, J., Geologic map of the Halaban quadrangle, sheet 23G, Kingdom of Saudi Arabia, scale 1:250,000, Geol. Map GM Saudi Arabia Dir. Gen. Miner. Resour., GM-46-A, 32 pp., 1979.

Dhellemmes, R., and J. Delfour, Geologic map of the Khaybar quadrangle, sheet 25D, Kingdom of Saudi Arabia, scale 1:250,000, Geol. Map GM Saudi Arabia Dir. Gen. Miner. Resour., GM-50-A, 24 pp., 1980.

Dixon, T.H., Gebel Dahanib, Egypt: A late Precambrian layered sill of komatiitic composition, Contrib. Mineral. Petrol., 76, 42-52, 1981.

El Bayoumi, R.M., Ophiolites and melange complex of Wadi Ghadir Area, Eastern Desert, Egypt, Pan-African Crustal Evolution in the Arabian-Nubian Shield, edited by A.R. Bakor et al., Bull. Fac. Earth Sci. King Abdulaziz Univ., 6, 329-342, 1984.

El Ramly, M.F., A new geological map for the basement rocks in the Eastern and Southwestern Deserts of Egypt, scale 1:1,000,000, Ann. Geol. Surv. Egypt, 2, 1-18, 1972.

El Ramly, M.F., and M.H. Hermina, Geologic map of the Aswan quadrangle, Egypt, scale 1:500,000, Egypt. Geol. Surv. and Min. Auth., Cairo, 1978.

El Ramly, M.F., R. Greiling, A. Kröner, and A.A.A. Rashwan, On the tectonic evolution of the Wadi Hafafit Area and environs, Eastern Desert of Egypt, Pan-African Crustal Evolution in the Arabian-Nubian Shield, edited by A.R. Bakor et al., Bull. Fac. Earth Sci. King Abdulaziz Univ., 6, 113-126, 1984.

El-Sharkawy, M.A., and R.M. El-Bayoumi, The ophiolites of Wadi Ghadir Area Eastern Desert, Egypt, Ann. Geol. Surv. Egypt, 9, 125-135, 1979.

El Shazly, E.M., On the classification of the Precambrian and other rocks of magmatic affiliation in Egypt, U.A.R., Int. Geol. Congr., 22, 88-101, 1964.

Freund, R., Plate tectonics of the Red Sea and East Africa, Nature, 228, 453, 1970.

Freund, R., Z. Garfunkel, I. Zak, M. Goldberg, T. Weissbrod, and B. Derin, The shear zone along the Dead Sea rift, Philos. Trans. R. Soc. London, Ser. A, 267, 107-130, 1970.

Garfunkel, Z., Internal structure of the Dead Sea leaky transform (rift) in relation to plate kinematics, Tectonophysics, 80, 81-108, 1981.

Girdler, R.W., and B.W. Darracott, African poles of rotation, Comments Earth Sci. Geophys., 2, 131-138, 1972.

Girdler, R.W., and P. Styles, Two stage Red Sea floor spreading, Nature, 247, 7-11, 1974.

Greene, D.C., Structural geology of the Quseir Area, Red Sea Coast, Egypt, M.Sc. thesis, 159 pp., Univ. of Mass.-Amherst, Amherst, 1984.

Greiling, R.O., Directions of Pan-African thrusting in the Eastern Desert of Egypt derived from lineation and strain data, in Current Research in African Earth Sciences, edited by G. Matheis and H. Schandelmeier, pp. 83-86, Balkema, Rotterdam, Netherlands, 1987.

Greiling, R., A. Kröner, and M.F. El Ramly, Structural interference patterns and their origin in the Pan-African basement of the southeastern desert of Egypt, in Precambrian Tectonics Illustrated, edited by A. Kröner, and R. Greiling, pp. 401-412, E. Schweizerbart'sche Verlagsbuchhandlung, Stuttgart, Federal Republic of Germany, 1984.

Greiling, R.O., A. Kröner, M.F. El Ramly, and A.A. Rashwan, Structural relationships between the southern and central parts of the Eastern Desert of Egypt: details of a fold and thrust belt, in The Pan-African Belt of Northeast Africa and Adjacent Areas, edited by S. El-Gaby and R.O. Greiling, pp. 121-145, Friedr. Vieweg, Braunschweig, Federal Republic of Germany, 1988.

Habib, M.E., A.A. Ahmed, and O.M. El Nady, Two orogenies in the Meatiq area of the central Eastern Desert, Egypt, Precambrian Res., 30, 83-111, 1985.

Johnson, P.R., A preliminary lithofacies map of the Saudi Arabian Shield: An interpretation of the lithofacies and lithostratigraphy of the late Proterozoic layered rocks of Saudi Arabia, Kingdom of Saudi Arabia, scale 1:1,000,000, Tech. Rec. RF-TR-03-2, Saudi Arabia Dep. Minist. for Miner. Resour., Jiddah, 1983.

Kemp, J., Geologic map of the Wadi al Ays quadrangle, sheet 25C, Kingdom of Saudi Arabia, scale 1:250,000, Geol. Map GM Saudi Arabia Dep. Minist. Miner. Resour., GM-53A, 39 pp., 1981.

Kemp, J., Y. Gros, and J.P. Prian, Geologic map of the Mahd Adh Dhahab quadrangle, sheet 23E, Kingdom of Saudi Arabia, scale 1:250,000, Geol. Map GM Saudi Arabia Dep. Minist. Miner. Resour., GM-64A, 39 pp., 1982.

Kröner, A., R. Greiling, T. Reischmann, I.M. Hussein, R.J. Stern, S. Dürr, J. Krüger, and M. Zimmer, Pan-African crustal evolution in the Nubian segment of northeast Africa, in Proterozoic Lithospheric Evolution, Geodyn. Ser., vol. 17, edited by A. Kröner, pp. 235-257, AGU, Washington D.C., 1987.

Letalenet, J., Geologic map of the Afif quadrangle, sheet 23F, Kingdom of Saudi Arabia, scale 1:250,000, Geol. Map GM Saudi Arabia Dir. Gen. Miner. Resour., GM-47-A, 20 pp., 1979.

McKenzie, D.P., D. Davies, and P. Molnar, Plate tectonics of the Red Sea and East Africa, Nature, 226, 243-248, 1970.

Moore, J.M., Tectonics of the Najd transcurrent fault system, Saudi Arabia, J. Geol. Soc. London, 136, 441-454, 1979.

Moore, J.M., and A.M. Al-Shanti, Structure and mineralization in the Najd fault system, Saudi Arabia, in Evolution and Mineralization of the Arabian-Nubian Shield, vol. 2, edited by A.M.S. Al-Shanti, pp. 17-28, Pergamon, Elmsford, N.Y., 1980.

Pellaton, C., Geologic map of the Yanbu al Bahr quadrangle, sheet 24C, Kingdom of Saudi Arabia, scale 1:250,000, Geol. Map GM Saudi Arabia Dir. Gen. Miner. Resour., GM-48-A, 16 pp., 1979.

Pellaton, C., Geologic map of the Al Madinah quadrangle, sheet 24D, Kingdom of Saudi Arabia, scale 1:250,000, Geol. Map GM Saudi Arabia Dep. Minist. Miner. Resour., GM-52A, 19 pp., 1981.

Pellaton, C., Geologic map of the Jabal al Buwanah quadrangle, sheet 24B, Kingdom of Saudi Arabia, scale 1:250,000, Geol. Map GM Saudi Arabia Dep. Minist. Miner. Resour., GM-62A, 10 pp., 1982a.

Pellaton, C., Geologic map of the Umm Lajj quadrangle, sheet 25B, Kingdom of Saudi Arabia, scale 1:250,000, Geol. Map GM Saudi Arabia Dep. Minist. Miner. Resour., GM-61A, 14 pp., 1982b.

Raleigh, C.B., and M.S. Paterson, Experimental deformations of serpentinite and its tectonic implications, J. Geophys. Res., 70, 3965-3985, 1965.

Raymond, L.A., Epilogue: Melanges: Future studies, Spec. Pap. Geol. Soc. Am., 198, 169-170, 1984.

Ries, A.C., R.M. Shackleton, R.H. Graham, and W.R. Fitches, Pan-African structures, ophiolites and melange in the Eastern Desert of Egypt: A traverse at 26^{0}N, J. Geol. Soc. London, 140, 75-95, 1983.

Rowan, L.C., P.H. Wetlaufer, A.F.H. Goetz,

F.C. Billingsley, and J.H. Stewart, Discrimination of rock types and detection of hydrothermally altered areas in south-central Nevada by the use of computer-enhanced ERTS images, U.S. Geol. Surv. Prof. Pap., 883, 35 pp. 1974.

Shackleton, R.M., A.C. Ries, R.H. Graham, and W.R. Fitches, Late Precambrian ophiolitic melange in the eastern desert of Egypt, Nature, 285, 472-474, 1980.

Shukri, N.M., and M. Lotfi, The geology of the Bir Barramiya area, Bull. Fac. Sci. Cairo Univ., 34, 83-130, 1955.

Smith, J.W., Geology of the Wadi Azlam quadrangle, sheet 27/36C, Kingdom of Saudi Arabia, scale 1:100,000, Geol. Map GM Saudi Arabia Dir. Gen. Miner. Resour., GM-36, 30 pp., 1979.

Stacey, J.S., and R.A. Agar, U-Pb isotopic evidence for the accretion of a continental microplate in the Zalm region of the Saudi Arabian Shield, J. Geol. Soc. London, 142, 1189-1203, 1985.

Steckler, M.S., Uplift and extension at the Gulf of Suez: Indications of induced mantle convection, Nature, 317, 135-139, 1985.

Stern, R.J., Petrogenesis and tectonic setting of late Precambrian ensimatic volcanic rocks, central Eastern Desert of Egypt, Precambrian Res., 16, 195-230, 1981.

Stern, R.J., The Najd fault system, Saudi Arabia and Egypt: A late Precambrian rift-related transform system?, Tectonics, 4, 497-511, 1985.

Stern, R.J., and C.E. Hedge, Geochronologic and isotopic constraints on late Precambrian crustal evolution in the Eastern Desert of Egypt, Am. J. Sci., 285, 97-127, 1985.

Stoeser, D.B., and V.E. Camp, Pan-African microplate accretion of the Arabian Shield, Geol. Soc. Am. Bull., 96, 817-826, 1985.

Sturchio, N.C., M. Sultan, and R. Batiza, Geology and origin of Meatiq dome, Egypt: A Precambrian metamorphic core complex?, Geology, 11, 72-76, 1983.

Sultan, M., R.E. Arvidson, and N.C. Sturchio, Mapping of serpentinites in the Eastern Desert of Egypt by using Landsat thematic mapper data, Geology, 14, 995-999, 1986.

Sultan, M., R.E. Arvidson, N.C. Sturchio, and E.A. Guinness, Lithologic mapping in arid regions with Landsat thematic mapper data: Meatiq dome, Egypt, Geol. Soc. Am. Bull., 99, 748-762, 1987.

Yilmaz, P.O., and J.C. Maxwell, An example of an obduction melange: The Alakir Cay unit, Antalya Complex, southwest Turkey, Spec. Pap. Geol. Soc. Am., 198, 139-150, 1984.

R.E. Arvidson, I.J. Duncan, and M. Sultan, Department of Earth and Planetary Sciences, McDonnell Center for the Space Sciences, Washington University, St. Louis, MO 63130.

B. El Kaliouby, Department of Geology, Faculty of Science, Ain Shams University, Abbassia, Cairo, Egypt.

R.J. Stern, Programs in Geosciences, University of Texas at Dallas, Richardson, TX 75083.

(Received February 22, 1988;
revised July 7, 1988;
accepted July 8, 1988.)